Multiple-pseudogap phases in the hydrogen-doped LaFeAsO system

A. Nakamura,[1] T. Shimojima,[1] T. Sonobe,[1] S. Yoshida,[1] K. Ishizaka,[1] W. Malaeb,[2,3] S. Shin,[2] S. Iimura,[4] S. Matsuishi,[5] and H. Hosono[4,5]

[1]*Quantum-Phase Electronics Center and Department of Applied Physics, The University of Tokyo, Hongo, Tokyo 113-8656, Japan*

[2]*Institute for Solid State Physics, The University of Tokyo, Kashiwa, Chiba 227-8581, Japan*

[3]*Physics Department, Faculty of Science, Beirut Arab University, Beirut 11-5020, Lebanon*

[4]*Laboratory for Materials and Structures, Tokyo Institute of Technology, Yokohama 226-8503, Japan*

[5]*Materials Research Center for Element Strategy, Tokyo Institute of Technology, Yokohama 226-8503, Japan*

(Received 26 April 2016; revised manuscript received 20 November 2016; published 2 February 2017)

The low-energy electronic structure of $LaFeAsO_{1-x}H_x$ ($0.0 \leqslant x \leqslant 0.60$), a system which exhibits two superconducting domes and antiferromagnetic orders in its phase diagram, is investigated by utilizing laser photoemission spectroscopy. From the precise temperature-dependent measurement of the spectra near the Fermi level, we find a suppression of the density of states with cooling, namely a pseudogap formation, for all doping range. The pseudogap gets suppressed on doping through the first superconducting dome regime to the higher-x region, whereas it tends to recover when further increasing x toward the second antiferromagnetic ordered phase. The systematic doping dependence indicates the different origins of pseudogaps in the low- and high-x regions, possibly related to the respective antiferromagnetic ground states residing at both ends of the phase diagram.

DOI: 10.1103/PhysRevB.95.064501

I. INTRODUCTION

Superconductivity in iron arsenides was discovered after F-doping antiferromagnetic LaFeAsO, with a maximum superconducting critical temperature (T_c) of 26 K [1]. The LnFeAsO (Ln = lanthanide) system tends to show high T_c as compared to other iron pnictide systems. Specifically, $SmFeAsO_{1-x}F_x$ displays one of the highest T_c among the iron pnictides [2]: 55 K at $x \sim 0.10$. Recent developments in the hydrogen substitution method [3–5] have greatly increased the electron-doping limit of the LnFeAsO system from $x \sim 0.2$ up to $x \sim 0.6$ [6]. In $LaFeAsO_{1-x}H_x$, a double-dome-shaped superconducting phase appears as a function of x as shown in Fig. 1: a low-x superconducting dome (SC1) at $x = 0.05-0.20$ with a maximum T_c of 29 K, and a high-x superconducting dome (SC2) at $x = 0.20-0.42$ with a maximum T_c of 36 K. These two superconducting domes seem to merge into one by applying high pressure [7] or by substituting the La ion by other lanthanides with smaller ion radius, such as Ce, Sm, and Gd [6]. In these cases, the maximum T_c becomes highly enhanced as compared to the $LaFeAsO_{1-x}H_x$ system in ambient pressure. Similar two-dome superconducting phase diagrams are also obtained in $LaFe(As_{1-x}P_x)O_{1-y}F_y$ [8] and $SmFeAs_{1-y}P_yO_{1-x}H_x$ [9], thus indicating the possible competition or cooperation of two different superconducting mechanisms that are inherent in the LnFeAsO system [10,11]. From this viewpoint, the investigation of SC1 and SC2 in $LaFeAsO_{1-x}H_x$ is important for revealing the mechanism that leads to high T_c value in the LnFeAsO family.

The phase diagram of $LaFeAsO_{1-x}H_x$ is further characterized by two antiferromagnetic (AF) states, namely AF1 ($x < 0.05$) and AF2 ($0.4 < x$), as shown in Fig. 1. AF2 has been clarified by nuclear magnetic resonance (NMR) [12,13], inelastic neutron scattering [14], and muon spin rotation (μSR) measurements [15]. The experiments show that AF1 and AF2 exhibit different magnetic ordering vectors, magnetic moments, and antiferromagnetic transition temperatures (T_N). It is also worth noting that there are two types of structural transitions on cooling below the structural phase transition temperature (T_S) from tetragonal to orthorhombic, whose doping dependence is similar to that of T_N. Such a rich phase diagram implies a possible variety of normal-state electronic properties as the background for SC1 and SC2 domes. According to density functional theory calculations [6,16–19], the $LaFeAsO_{1-x}H_x$ system has hole and electron Fermi surfaces at the center and the corners of the Brillouin zone, respectively, which are composed of multiple Fe 3d orbitals. Upon electron doping from $x = 0.0$ to $x = 0.40$, the shape of the Fermi surface drastically changes. Consequently, the spin fluctuations connecting the Fermi surfaces of YZ/ZX orbitals are expected to develop in the SC1 region while those between the Fermi surfaces of X^2-Y^2 orbitals should become dominant in SC2 [19,20] (X/Y and Z correspond to the tetragonal axes a^T and c^T). Theoretical studies considering both spin and orbital susceptibilities, on the other hand, have proposed a simultaneous evolution of the spin and orbital fluctuations for both SC1 and SC2 phases [18].

Experimentally, photoemission spectroscopy studies on F-doped $LaFeAsO_{1-x}F_x$ ($0 \leqslant x \leqslant 0.14$) were employed soon after its discovery, to investigate the normal-state electronic structure [21–24]. Some of them reported a pseudogap evolving from a temperature above the SC1 phase transition, which was attributed to the precursor of the antiferromagnetic gap or the antiferromagnetic spin fluctuations [22]. However, there has been no report on $LaFeAsO_{1-x}H_x$ system until now, where the high-x SC2 dome is available. Recently, an NMR measurement revealed that the spin relaxation rate $1/T_1T$ gets strongly suppressed with cooling below T^* ($T^* > T_N$) in the heavily doped regime ($x > 0.4$) [25]. Such a deviation from the Curie-Weiss behavior may suggest the possible emergence of a pseudogap also in the SC2 region. Considering that the antiferromagnetic ordered states at $x \sim 0.0$ and $x \sim 0.50$ show different magnetic and structural properties, the systematic investigation of the electronic structure in a wide range of the phase diagram will provide information on the origin of the two-dome superconductivity and its possible relation to the pseudogaps.

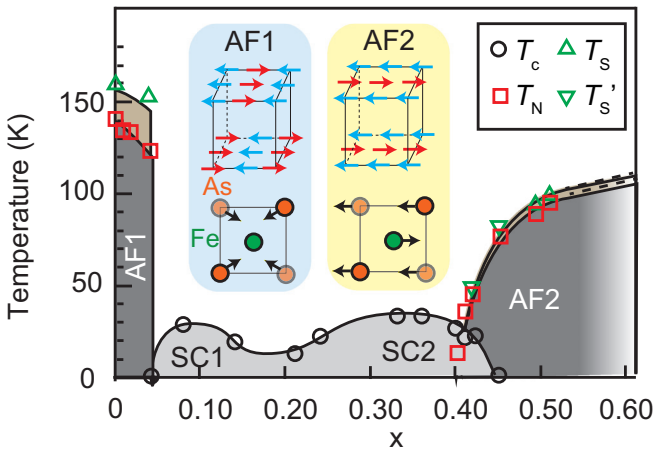

FIG. 1. Phase diagram of $LaFeAsO_{1-x}H_x$ [6,12,13,15]. T_S' indicates the T where the c axis length starts to increase, as observed by x-ray diffraction measurements [15]. The magnetic structure and the displacements of the Fe and As atoms in the AF1 and AF2 ordered phases are also shown in the inset [15].

In this study, we use angle-integrated photoemission spectroscopy (AIPES) to investigate polycrystalline $LaFeAsO_{1-x}H_x$ in a wide range of temperature ($6 \leqslant T \leqslant 300$ K) and compositions ($0.0 \leqslant x \leqslant 0.60$). Though the single crystals of $LaFeAsO_{1-x}H_x$ suitable for angle-resolved photoemission spectroscopy (ARPES) are not yet available at present, the T-dependent density of states (DOS) near the Fermi level (E_F) can be precisely acquired by using laser AIPES. We newly find a pseudogap in the high-x region ($x = 0.35$-0.60), evolving from T above SC2 and AF2 phase transitions. The doping dependence of the pseudogap in the SC2-AF2 region is clearly distinguished from the pseudogaps in the low-x AF1-SC1 region. The doping dependence of the pseudogap temperature (T_{PG}) in the whole phase diagram indicates that these pseudogaps originate from respective electronic ground states of the AF1 ($x \sim 0.0$) and AF2 ($x \sim 0.50$) phases, respectively, which may also be crucial for the occurrence of two-dome superconductivity.

II. METHODS

Polycrystalline $LaFeAsO_{1-x}H_x$ ($x = 0.0, 0.10, 0.20, 0.35, 0.50, 0.60$) samples were synthesized as described in Ref. [6]. For pseudogap measurements, high-energy-resolution laser AIPES measurements were performed with a spectrometer built using a VG-Scienta R4000 electron analyzer and an ultraviolet laser of 6.994 eV as a photon source at the Institute for Solid State Physics, University of Tokyo [26,27]. The energy resolution was set to about 6 meV to obtain a high count rate of photoelectrons. For the AIPES measurements for $x = 0.35$ sample at low T (< 70 K), we employed the fourth-harmonic generation of Ti:sapphire laser radiation ($h\nu = 6.42$ eV) and VG-Scienta R4000WAL electron analyzer with the energy resolution of 3 meV at the University of Tokyo [28]. While previous ARPES studies reported the strong surface effect for the 1111 systems [29,30], we use the low-energy photoelectrons with the long escape depth [31] which is expected to be bulk sensitive. The E_F of the samples was referenced to that of a gold film evaporated onto the sample holder, within an accuracy of ± 0.3 meV. All the polycrystalline samples were fractured *in situ* at 200 K in an ultrahigh vacuum better than 1×10^{-10} Torr. We confirmed the reproducibility of the T-dependent AIPES spectrum by measuring it during a T cycle.

III. RESULTS AND DISCUSSION

Figure 2 shows the photoemission spectra near the E_F at $x = 0.0$ (AF1), 0.10 (SC1), 0.35 (SC2), and 0.50 (AF2). The raw spectra shown in Figs. 2(a)–2(d) were normalized by the spectral intensity integrated between the binding energies (E_B) of 120 and 130 meV. All the spectra show an almost linear slope toward the higher E_B, being consistent with previous photoemission measurements on F-doped $LaFeAsO_{1-x}F_x$ [21–24]. Apparently the spectral intensity at the E_F decreases with cooling for all compositions. To remove the contributions of the Fermi-Dirac (FD) distribution and focus on the T dependence of DOS, the AIPES spectra were divided by FD distribution function, as shown in Figs. 2(e)–2(h). The thin blue curves overlaid on respective red curves are those obtained at the lowest T, i.e., 12 K for $x = 0.0$ (AF1), 7 K for $x = 0.10$ (SC1), 8 K for $x = 0.35$ (SC2), and 10 K for $x = 0.50$ (AF2). The black triangles indicate the energy position where the thin blue curves deviate from the red curves. Here we can distinguish a suppression of the DOS near the E_F with cooling, for all the samples.

When we look at the energy positions of the triangle markers as a function of T, we notice two different behaviors. At high T, the black triangles show a monotonic decrease of the energy scale with cooling. In contrast, below a certain T [here named T_0, see Figs. 2(e)–2(h) for their values], the positions of the black triangle markers become nearly T independent. The spectral suppression with the k_BT-dependent (k_B: Boltzmann constant) energy scale obtained at $T > T_0$ was also reported in a previous photoemission study on $LaFeAsO_{1-x}F_x$ [21]. Since the energy scale is nearly proportional to k_BT, this observation was discussed in terms of the thermal effect in the semimetal-like electronic structure of the compound [21]. On the other hand, the spectral suppression with the T-independent energy scale occurring at $T < T_0$ is similar to the pseudogap formation in cuprates and pnictides [32,33].

Here we focus on the low T region ($T < T_0$) where the k_BT-dependent features are not dominant and can be more or less excluded. The T dependence of the raw spectra below T_0 is shown in Figs. 3(a)–3(d). The insets show the magnified spectra at the E_F. The crossing points of the AIPES spectra are located below the E_F as indicated by the red bars. We also find that the spectral intensity at the E_F gradually decreases on cooling. These spectral features are indicative of the clear leading edge shifts for all samples. The AIPES spectra divided by the FD distribution functions were further normalized by those at T_0 to evaluate their T dependence as shown in Figs. 3(e)–3(h). We confirmed that this normalization process does not affect the results even when T_0 is intentionally changed within ± 10 K, for all doping range. For $x = 0$ [Fig. 3(e)], the spectra show a slightly gapped area gradually appearing at 170 K on cooling, in the energy range up to ~ 30 meV. We also find that the integrated area

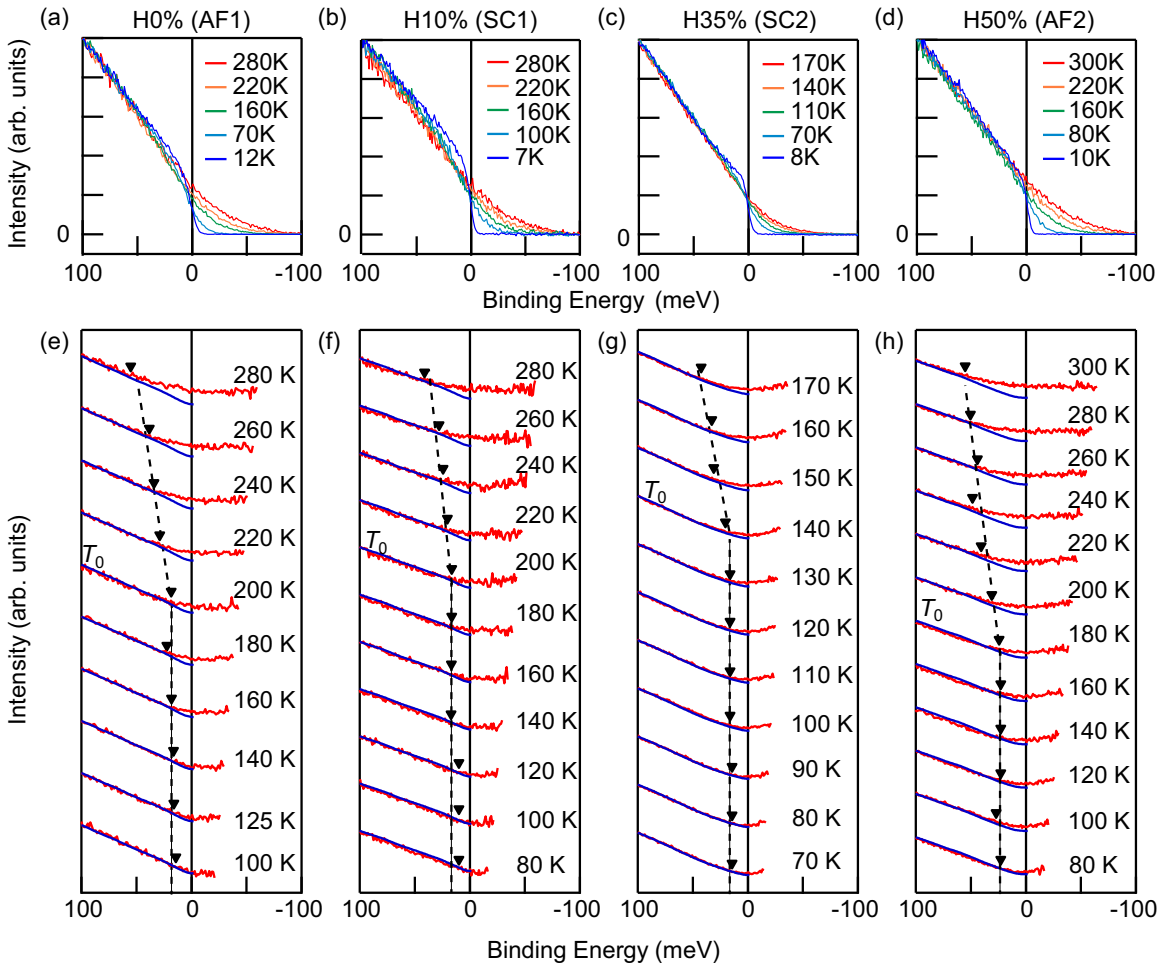

FIG. 2. (a)–(d) T dependence of AIPES spectra near the E_F for $x = 0.0$ (AF1), 0.10 (SC1), 0.35 (SC2), and 0.50 (AF2), respectively. (e)–(h) T dependence of the AIPES spectra divided by the FD distribution function for $x = 0.0$, 0.10, 0.35, and 0.50, respectively. The red curves show the data at respective T, whereas the blue curves denote those at the lowest T; 12 K for $x = 0.0$, 7 K for $x = 0.10$, 8 K for $x = 0.35$, and 10 K for $x = 0.50$, respectively. The black triangles indicate the energy where the red curves deviate from the blue curves. The black broken lines are the guides for the eyes.

from the E_F to the E_B of 100 meV is not conserved when the T is varied. This suggests that the decreased spectral weight is redistributed over a wide energy range, similar to the case of Kondo insulators [34].

The estimated energy scale of the gaplike structure, displayed in Fig. 4(a), is also indicated by the gray lines in Fig. 3(e). This energy scale is T independent, being distinctly different from the $k_B T$-dependent feature appearing at higher T. Considering that the parent LaFeAsO ($x = 0$) is known to exhibit an antiferromagnetic transition at 140 K, the gaplike depression in the DOS evolving already at 160 K should not correspond exactly to the antiferromagnetic gap itself. We identify this gaplike feature as a pseudogap (PG1H). For the estimation of the characteristic T of the pseudogap (T_{PG1H}), we plot the gapped areas in Fig. 4(g), which are calculated by integrating the normalized FD-divided spectra [Fig. 3(e)] within the pseudogap energy Δ_{PG1H}, which is shown in Fig. 4(a). While the estimation of T_{PG1H} is difficult because of the crossoverlike T dependence of the pseudogap, here we determine the lower and upper limits of T_{PG1H} as T where the gapped area becomes larger than its experimental error and smaller than half of the experimental error, respectively. T_{PG1H} for $x = 0.0$ thus estimated is 172.5 ± 7.5 K. Regarding the antiferromagnetic transition at 140 K, we cannot separately find any additional feature indicative of the antiferromagnetic gap, which was also not observed in a previous ARPES study on LaFeAsO [29]. Here we note that the T range of the pseudogap formation ($T < 180$ K) is significantly lower as compared to the anomalous band shifts continuously evolving up to 300 K as reported in several Fe-pnictide systems [35,36]. This fact seems to indicate that these two phenomena are different in origin, which should be further investigated especially by ARPES for understanding the anomalous T-dependent electronic structures.

In the case of $x = 0.10$, the optimal composition of SC1, we find the evolution of the pseudogap below 180 ± 10 K with an energy scale of $\Delta_{PG1H} = \sim 40$ meV as shown in Figs. 3(f), 4(b), and 4(h). The spectrum at 40 K in Fig. 4(b) shows an additional kink structure at ~ 20 meV, which may correspond to the smaller pseudogap with lower energy and temperature (PG1L) as reported in the previous study on $LaFeAsO_{1-x}F_x$ [24]. A similar pseudogap is also observed for $x = 0.20$, showing

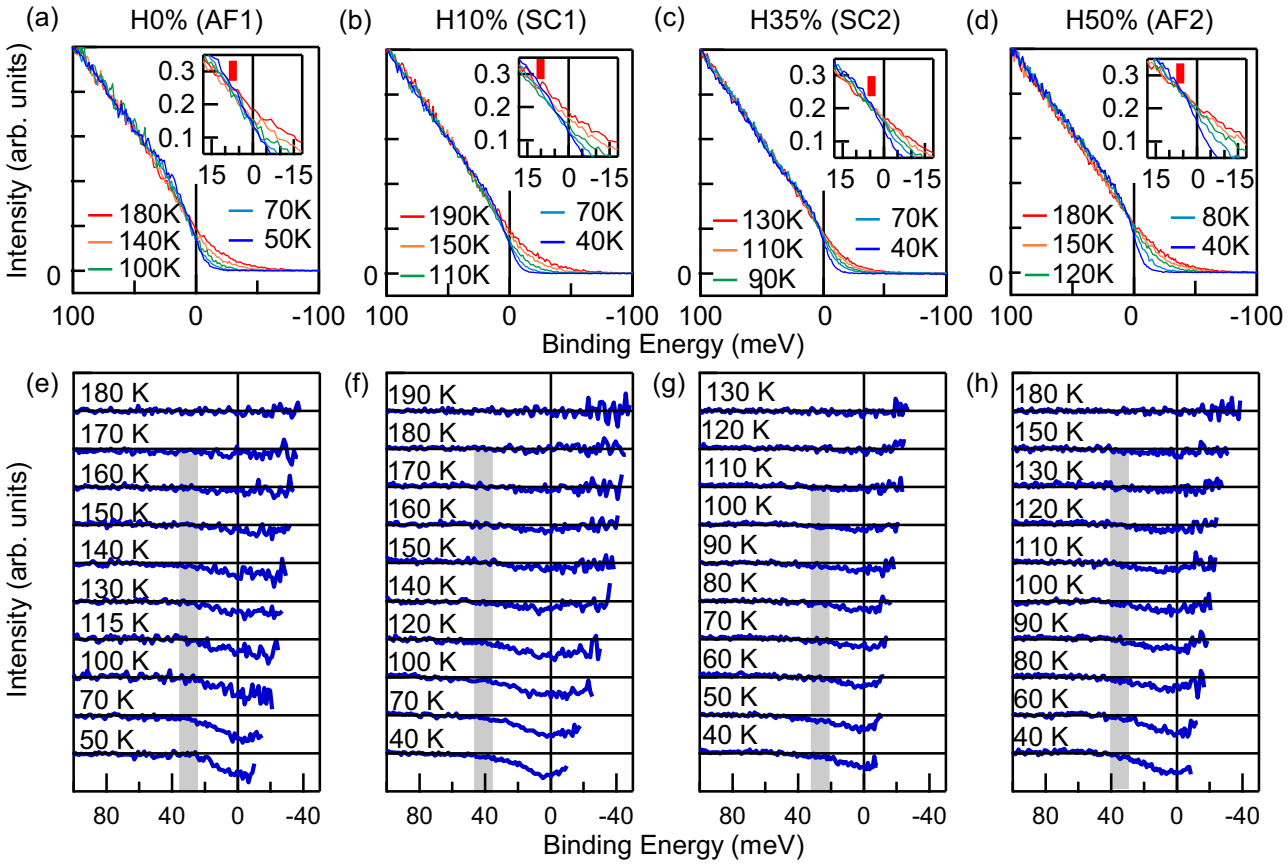

FIG. 3. (a)–(d) T dependence of AIPES spectra for $x = 0.0$, 0.10, 0.35, and 0.50, respectively. The insets show the magnification spectra near the E_F. The red bars represent the crossing points of the AIPES spectra. (e)–(h) The FD-divided AIPES spectra normalized at T_0 obtained for $x = 0.0$, 0.10, 0.35, and 0.50, respectively. The gray lines indicate the energy scale of the pseudogap Δ_{PG}.

$T_{PG1H} = 160 \pm 10$ K and $\Delta_{PG1H} = \sim 30$ meV [Figs. 4(c) and 4(i)]. Throughout the AF1-SC1 region, PG1H is characterized by $T_{PG1H} = 160-180$ K and $\Delta_{PG1H} = 30-40$ meV, and seems to be robust against H doping. The nonmonotonic doping dependence of T_{PG1H} and Δ_{PG1H} in this region may be suggesting some yet unknown mechanism of correlation effect in SC1, which remains to be further elucidated.

For the SC2 and AF2 regions ($x > 0.35$), we also find the pseudogap evolution on cooling (PG2). As shown in Figs. 3(g), 4(d), and 4(j), the PG2 with $\Delta_{PG2} = \sim 25$ meV starts to evolve at $T_{PG2} = 115 \pm 5$ K for $x = 0.35$ (SC2), which is clearly suppressed as compared to PG1H. However, the observed pseudogap feature seems to be enhanced with increasing x to 0.6, as shown in Figs. 3(g), 3(h), 4(d)–4(f), and 4(j)–4(l). The energy and T scales of the pseudogap are $\Delta_{PG2} = \sim 35$ meV and $T_{PG2} = 160 \pm 10$ K for $x = 0.50$, and $\Delta_{PG2} = \sim 45$ meV and $T_{PG2} = 150 \pm 10$ K for $x = 0.60$. In addition to the T_{PG2} and Δ_{PG2}, the gapped areas are also enhanced in AF2 region as compared to $x = 0.35$. Thus, PG2 for the SC2-AF2 region clearly shows a doping-dependent behavior different from PG1H (AF-SC1 region). According to the μSR measurements [15], T_N at $x = 0.50$ (AF2) was estimated to be approximately 90 K. The observed T_{PG2} is again higher than T_N, which indicates that the gap features observed at $x = 0.50$ and 0.60 are not directly associated with the antiferromagnetic gap itself.

Here we focus on the T dependence of the AIPES spectra across T_c (36 K) for $x = 0.35$ (SC2). As shown in Fig. 5(a), we observed a decrease in the spectral weight near the E_F with lowering T while it is absent in the spectra for polycrystalline gold [Fig. 5(b)]. The T-dependent spectral DOS are analyzed by the FD-divided spectra as shown in Figs. 5(c) and 5(d). For the quantitative analysis, we show the T dependencies of the spectral DOS at several E_B in Fig. 5(e), which are obtained from the spectra in Fig. 5(c). The spectral DOS at $E_B \geqslant 4$ meV exhibits a T linear behavior from 70 to 13 K possibly due to the evolution of the 25 meV pseudogap [Fig. 4(d)]. We also find that the spectral DOS at $E_B < 4$ meV exhibits an additional decrease below T_c. This spectral depression at low T may be reflecting the superconducting gap opening, i.e., the bulk electronic properties in the $LaFeAsO_{1-x}H_x$ system.

Based on the present results, all T_{PG} values are summarized in the phase diagram in Fig. 6. For comparison, the T_{PG} values for F-doped samples are also displayed by the open squares and open triangles, taken from Refs. [22] and [24], respectively. We observed PG1H in the low-x AF1 and SC1 regions, with $T_{PG1H} = 160-180$ K and $\Delta_{PG1H} = 30-40$ meV. T_{PG} seems to be higher than those reported in Ref. [22] (PG1L, the black dashed line), which may be due to the two types of pseudogaps reported for F-doped LaFeAsO in AF1 and SC1 regions [24]. In addition to the PG1H, we observed PG2 in the high-x SC2 and AF2 regions, which becomes enhanced with increasing x from SC2 to AF2. This suggests that the PG2 originates not from AF1, but from another electronic ground state at the higher doping region.

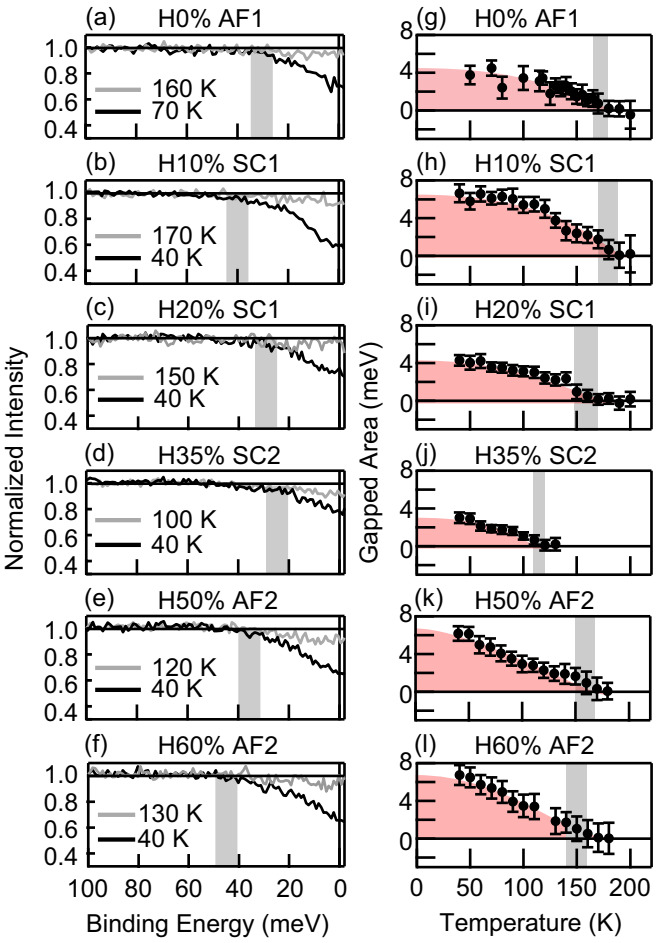

FIG. 4. (a)–(f) The FD-divided AIPES spectra normalized at T_0 obtained for $x = 0.0$, 0.10, 0.20, 0.35, 0.50, and 0.60, respectively. The gray vertical bars show the energy scales of the pseudogaps Δ_{PG1} and Δ_{PG2}. (g)–(l) Temperature dependence of the gapped areas for $x = 0.0$, 0.10, 0.20, 0.35, 0.50, and 0.60, respectively. These gapped areas are calculated by integrating the normalized FD-divided spectra from Δ_{PG} to E_F. The gray vertical bars indicate the characteristic temperatures of the pseudogaps T_{PG1H} and T_{PG2}.

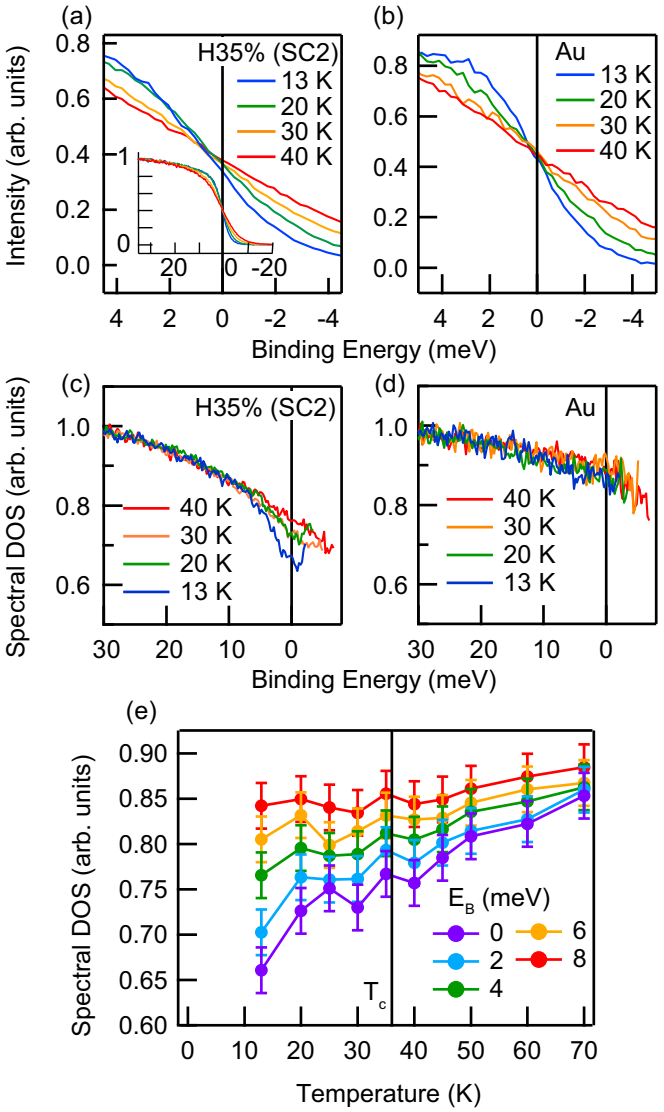

FIG. 5. (a) and (b) The AIPES spectra obtained at several T across T_c for $x = 0.35$ (SC2) and polycrystalline gold, respectively. These spectra were normalized by the spectral intensity integrated between the binding energies of 30 and 40 meV. (c) and (d) The FD-divided AIPES spectra for $x = 0.35$ (SC2) and polycrystalline gold, respectively. (e) The T dependence of the spectral DOS at $E_B = 0$, 2, 4, 6, and 8 meV obtained for $x = 0.35$. The black solid line represents the T_c (36 K).

The pseudogaps in iron pnictides have been experimentally and theoretically discussed in relation to the spin/orbital fluctuations. Considering the smooth doping dependence of T_{PG1L} that follows after T_N in AF1 phase, the spin fluctuation derived from hole and electron Fermi surface nesting is a possible candidate for the origin of PG1L, as raised in the previous photoemission studies [22,24]. PG1H, on the other hand, had been discussed in association with the structural phase transition in F-doped LaFeAsO [24]. An electronic nematicity evolving around 175 K detected by in-plane resistivity [37] may also be playing a crucial role for the pseudogap formation, as mentioned in Ref. [33]. Regarding PG2, the enhancement of T_{PG2} toward high x implies that PG2 is related to the AF2 phase. Such pseudogap formation may correspond to the evolution of the spin/orbital fluctuations particular to the SC2 region, as suggested by theoretical studies [6,16–20]. Actually, spin fluctuations with different wave numbers at $x = 0.0$ and $x = 0.40$ have been detected by inelastic neutron scattering measurements [14], while both types of fluctuations are suppressed in the middle ($x \sim 0.20$) region. The NMR measurement, on the other hand, proposed that the orbital degrees of freedom or the orbital ordering may be in charge of the pseudogap behavior in the SC2 region [25]. To more solidly clarify the PG1 and PG2 states, and discuss how they overlap or crossover to each other, the precise electronic structures and dynamical magnetic properties using single crystals remain to be investigated in the future.

IV. CONCLUSION

In summary, we performed laser AIPES on $LaFeAsO_{1-x}H_x$ ($0.0 \leqslant x \leqslant 0.60$) for a wide T region, and observed peculiar pseudogaps of energy scales 25–45 meV existing throughout the phase diagram. While the T_{PG} and Δ_{PG} decrease with

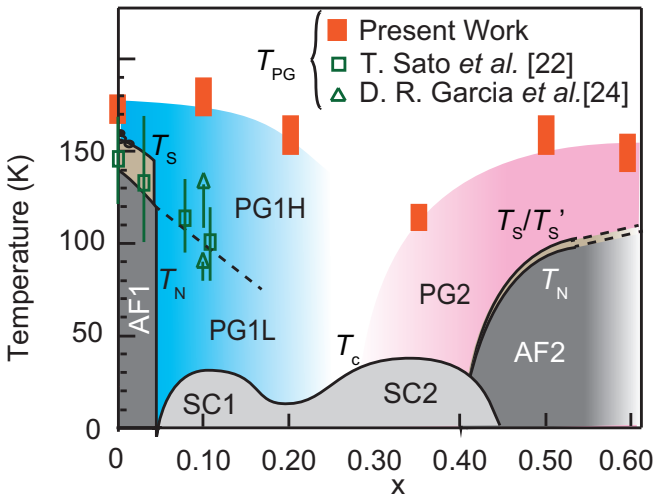

FIG. 6. Phase diagram showing the pseudogaps of $LaFeAsO_{1-x}H_x$. The orange bars represent the T_{PG} values of H-doped LaFeAsO, as estimated from the present laser-AIPES measurements. The open squares and triangles represent T_{PG} values obtained by the previous AIPES studies on F-doped LaFeAsO [22,24]. The T_c, T_N, T_S, and T_S' values were taken from Refs. [6] and [15].

increasing x through the PG1 region, it becomes higher as x exceeds 0.35 in the PG2 region. The qualitative difference of the doping dependence between PG1 and PG2 indicates the distinct origins for respective pseudogap states, possibly related to the two antiferromagnetic phases AF1 ($x \sim 0.0$) and AF2 ($x \sim 0.5$), respectively. The present result may indicate that there are two types of spin/orbital fluctuations existing in the $LaFeAsO_{1-x}H_x$ system, which should lead to the two pseudogap phases and possibly also to the two superconducting domes.

ACKNOWLEDGMENTS

We thank S. Ideta for valuable discussions. A. Nakamura acknowledges support by Advanced Leading Graduate Course for Photon Science (ALPS) at the University of Tokyo. This research was partly supported by the Photon Frontier Network Program of the MEXT; Research Hub for Advanced Nano Characterization, The University of Tokyo, supported by MEXT, Japan; and Grant-in-Aid for Scientific Research from JSPS, Japan (KAKENHI 15H03683, 16K13815, and 15H03687). The research at Tokyo Tech was supported by MEXT grant for Element Strategy Initiative to form a research core.

[1] Y. Kamihara, T. Watanabe, M. Hirano, and H. Hosono, J. Am. Chem. Soc. **130**, 3296 (2008).
[2] Y. Kamihara, T. Nomura, M. Hirano, J. E. Kim, K. Kato, M. Takata, Y. Kobayashi, S. Kitao, S. Higashitaniguchi, Y. Yoda, M. Seto, and H. Hosono, New J. Phys. **12**, 033005 (2010).
[3] T. Hanna, Y. Muraba, S. Matsuishi, N. Igawa, K. Kodama, S. I. Shamoto, and H. Hosono, Phys. Rev. B **84**, 024521 (2011).
[4] S. Matsuishi, T. Hanna, Y. Muraba, S. W. Kim, J. E. Kim, M. Takata, S. I. Shamoto, R. I. Smith, and H. Hosono, Phys. Rev. B **85**, 014514 (2012).
[5] H. Hosono and S. Matsuishi, Curr. Opin. Solid State Mater. Sci. **17**, 49 (2013).
[6] S. Iimura, S. Matuishi, H. Sato, T. Hanna, Y. Muraba, S. W. Kim, J. E. Kim, M. Takata, and H. Hosono, Nat. Commun. **3**, 943 (2012).
[7] H. Takahashi, H. Soeda, M. Nukii, C. Kawashima, T. Nakanishi, S. Iimura, Y. Muraba, S. Matsuishi, and H. Hosono, Sci. Rep. **5**, 7829 (2015).
[8] H. Mukuda, F. Engetsu, K. Yamamoto, K. T. Lai, M. Yashima, Y. Kitaoka, A. Takemori, S. Miyasaka, and S. Tajima, Phys. Rev. B **89**, 064511 (2014).
[9] S. Matsuishi, T. Maruyama, S. Iimura, and H. Hosono, Phys. Rev. B **89**, 094510 (2014).
[10] S. Miyasaka, A. Takemori, T. Kobayashi, S. Suzuki, S. Saijo, and S. Tajima, J. Phys. Soc. Jpn. **82**, 124706 (2013).
[11] J. Ishida, S. Iimura, S. Matsuishi, and H. Hosono, J. Phys. Condens. Matter **26**, 435702 (2014).
[12] N. Fujiwara, S. Tsutsumi, S. Iimura, S. Matsuishi, H. Hosono, Y. Yamakawa, and H. Kontani, Phys. Rev. Lett. **111**, 097002 (2013).
[13] N. Fujiwara, S. Iimura, S. Matsuishi, H. Hosono, Y. Yamakawa, and H. Kontani, J. Supercond. Nov. Magn. **27**, 933 (2014).
[14] S. Iimura, S. Matsuishi, M. Miyakawa, T. Taniguchi, K. Suzuki, H. Usui, K. Kuroki, R. Kajimoto, M. Nakamura, Y. Inamura, K. Ikeuchi, S. Ji, and H. Hosono, Phys. Rev. B **88**, 060501 (2013).
[15] M. Hiraishi, S. Iimura, K. M. Kojima, J. Yamaura, H. Hiraka, K. Ikeda, P. Miao, Y. Ishikawa, S. Torii, M. Miyazaki, I. Yamauchi, A. Koda, K. Ishii, M. Yoshida, J. Mizuki, R. Kadono, R. Kumai, T. Kamiyama, T. Otomo, Y. Murakami, S. Matsuishi, and H. Hosono, Nat. Phys. **10**, 300 (2014).
[16] K. Suzuki, H. Usui, K. Kuroki, S. Iimura, Y. Sato, S. Matsuishi, and H. Hosono, J. Phys. Soc. Jpn. **82**, 083702 (2013).
[17] Y. Yamakawa, S. Onari, H. Kontani, N. Fujiwara, S. Iimura, and H. Hosono, Phys. Rev. B **88**, 041106 (2013).
[18] S. Onari, Y. Yamakawa, and H. Kontani, Phys. Rev. Lett. **112**, 187001 (2014).
[19] K. Suzuki, H. Usui, S. Iimura, Y. Sato, S. Matsuishi, H. Hosono, and K. Kuroki, Phys. Rev. Lett. **113**, 027002 (2014).
[20] H. Arai, H. Usui, K. Suzuki, Y. Fuseya, and K. Kuroki, Phys. Rev. B **91**, 134511 (2015).
[21] Y. Ishida, T. Shimojima, K. Ishizaka, T. Kiss, M. Okawa, T. Togashi, S. Watanabe, X.-Y. Wang, C.-T. Chen, Y. Kamihara, M. Hirano, H. Hosono, and S. Shin, Phys. Rev. B **79**, 060503 (2009).
[22] T. Sato, K. Nakayama, Y. Sekiba, T. Arakane, K. Terashima, S. Souma, T. Takahashi, Y. Kamihara, M. Hirano, and H. Hosono, J. Phys. Soc. Jpn. **77**, 65 (2008).
[23] W. Malaeb, T. Yoshida, T. Kataoka, A. Fujimori, M. Kubota, K. Ono, H. Usui, K. Kuroki, R. Arita, H. Aoki, Y. Kamihara, M. Hirano, and H. Hosono, J. Phys. Soc. Jpn. **77**, 093714 (2008).
[24] D. R. Garcia, C. Jozwiak, C. G. Hwang, A. Fedorov, S. M. Hanrahan, S. D. Wilson, C. R. Rotundu, B. K. Freelon, R. J. Birgeneau, E. Bourret-Courchesne, and A. Lanzara, Phys. Rev. B **78**, 245119 (2008).

[25] R. Sakurai, N. Fujiwara, N. Kawaguchi, Y. Yamakawa, H. Kontani, S. Iimura, S. Matsuishi, and H. Hosono, Phys. Rev. B **91**, 064509 (2015).

[26] T. Kiss, T. Shimojima, K. Ishizaka, A. Chainani, T. Togashi, T. Kanai, X.-Y. Wang, C.-T. Chen, S. Watanabe, and S. Shin, Rev. Sci. Instrum. **79**, 023106 (2008).

[27] T. Shimojima, K. Okazaki, and S. Shin, J. Phys. Soc. Jpn. **84**, 072001 (2015).

[28] J. Omachi, K. Yoshioka, and M. Kuwata-Gonokami, Opt. Express **20**, 23542 (2012).

[29] L. X. Yang, B. P. Xie, Y. Zhang, C. He, Q. Q. Ge, X. F. Wang, X. H. Chen, M. Arita, J. Jiang, K. Shimada, M. Taniguchi, I. Vobornik, G. Rossi, J. P. Hu, D. H. Lu, Z. X. Shen, Z. Y. Lu, and D. L. Feng, Phys. Rev. B **82**, 104519 (2010).

[30] C. Liu, Y. Lee, A. D. Palczewski, J.-Q. Yan, T. Kondo, B. N. Harmon, R. W. McCallum, T. A. Lograsso, and A. Kaminski, Phys. Rev. B **82**, 075135 (2010).

[31] M. P. Seah and W. A. Dench, Surf. Interface Anal. **1**, 2 (1979).

[32] T. Sato, H. Matsui, S. Nishina, T. Takahashi, T. Fujii, T. Watanabe, and A. Matsuda, Phys. Rev. Lett. **89**, 067005 (2002).

[33] T. Shimojima, T. Sonobe, W. Malaeb, K. Shinada, A. Chainani, S. Shin, T. Yoshida, S. Ideta, A. Fujimori, H. Kumigashira, K. Ono, Y. Nakashima, H. Anzai, M. Arita, A. Ino, H. Namatame, M. Taniguchi, M. Nakajima, S. Uchida, Y. Tomioka, T. Ito, K. Kihou, C. H. Lee, A. Iyo, H. Eisaki, K. Ohgushi, S. Kasahara, T. Terashima, H. Ikeda, T. Shibauchi, Y. Matsuda, and K. Ishizaka, Phys. Rev. B **89**, 045101 (2014).

[34] H. Kumigashira, T. Sato, T. Yokoya, T. Takahashi, S. Yoshii, and M. Kasaya, Phys. Rev. Lett. **82**, 1943 (1999).

[35] R. S. Dhaka, S. E. Hahn, E. Razzoli, R. Jiang, M. Shi, B. N. Harmon, A. Thaler, S. L. Bud'ko, P. C. Canfield, and A. Kaminski, Phys. Rev. Lett. **110**, 067002 (2013).

[36] V. Brouet, P.-H. Lin, Y. Texier, J. Bobroff, A. Taleb-Ibrahimi, P. Le Fèvre, F. Bertran, M. Casula, P. Werner, S. Biermann, F. Rullier-Albenque, A. Forget, and D. Colson, Phys. Rev. Lett. **110**, 167002 (2013).

[37] A. Jesche, F. Nitsche, S. Probst, T. Doert, P. Müller, and M. Ruck, Phys. Rev. B **86**, 134511 (2012).